

0168-9002/91/\$03.50 © 1991 – Elsevier Science Publishers B.V. (North-Holland)

3. Short-term gain variations

We have extensively studied the rate effect for 12 XP2008 PMTs at a high voltage supply of -1680 V, namely 80% of the maximum allowed by the manufacturer. Some tests were also done with PMTs supplied at lower and higher voltages, to study the influence of a change in the HV supply on the rate effect.

Gain variations have been measured with respect to a reference state, in which one light pulse from the RLED corresponds to $N_R \sim 300$ photoelectrons, and the count rate is $\nu_R = 100$ Hz. Such light pulses correspond approximately to those due to a minimum ionising particle, crossing 1 cm of NE102 scintillator. We have checked the effect of changing ν_R and Q_R within a factor of 2–3 to obtain the same I_R , with no difference in the gain of the PMTs. We shall indicate as G_0 ($\sim 10^6$) the PMT gain in this reference state.

We have studied gain variations between this reference low current state and several states that we characterise by the expected mean anode current in the absence of rate-related gain variations $I = I_R + I_B$, where $I_B = eN_B G_0 \nu_B$.

The maximum burst mean anode current provided by the BLED ($I = 80 \mu\text{A}$) is well below the maximum allowed by the manufacturer ($I_{\text{max}} = 200 \mu\text{A}$), and still much lower than the current flowing in the voltage divider. Nevertheless, to check the presence of problems related to a redistribution of interdynode potentials, we have repeated all measurements on one PMT, supplying the voltage to the last two dynodes by means of an external high-current power supply. No difference was found in the whole range of measurements up to $I = 80 \mu\text{A}$ and to a voltage of -1800 V between those two HV supply configurations.

To study the rate effect in realistic conditions, we simulated a cycle similar to the experimental conditions at present accelerators, in which particles are spilled during a few-seconds burst, followed by an idle period. We define as “short-term” rate effect the gain variation observed in such cycles: the cycle chosen is composed of a 10 s burst, followed by a 50 s recovery time.

When the light amplitude and/or the rate on the photocathode are raised, the gain of the PMTs increases exponentially with time, reaching a new stable value after a few tenths of a second. The gain stays stable during the high-current burst, and an exponential recovery is observed when the excitation is turned off at the end of the burst (fig. 4).

Since typical times to be measured (i.e. those necessary to reach and leave the excited state) are much faster than the time necessary to acquire one event, and to transfer it to mass memory, we have used a sampling technique. This is required by the fact that the DAQ system run by CAVIAR needs more than 500 ms between two ADC readings to transfer the data to mass

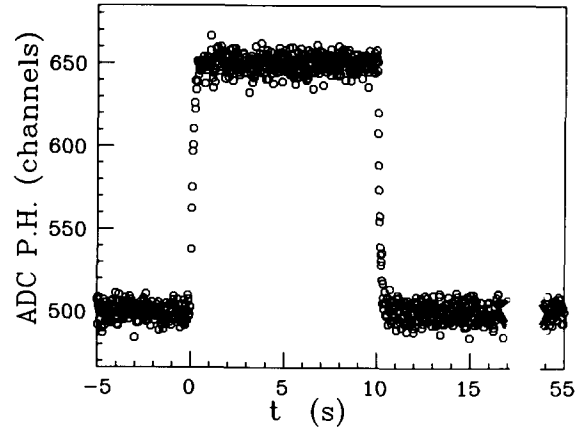


Fig. 4. A typical example of PMT gain behaviour during the cycle adopted.

memory (i.e. VAX 11/780 or floppy disc). To overcome this bound, we sampled the 10 s period several times, shifting each time a hardware-generated delay. A circuit (shown in fig. 5) allows to delay the external trigger driving the BLED by 50 to 500 ms; readout of the ADC immediately after both start and end of the high-current burst is thus possible. Measurements collected are superimposed in the off-line analysis, and the final curve ΔG vs t is obtained (fig. 6).

The gain variation is defined as

$$\Delta G = \frac{\langle \text{ADC} - \text{PED} \rangle - \langle \text{ADC}_0 - \text{PED}_0 \rangle}{\langle \text{ADC}_0 - \text{PED}_0 \rangle},$$

where ADC_0 and PED_0 are the output signal and pedestal values of the RLED light pulse at the reference state ($I = I_R$), and ADC , PED are the same quantities during the high-current burst. Pedestals are measured in dedicated runs in order to correct for frequency-dependent pedestals shifts.

The gain variation has been investigated at various mean anode currents

$$I = Q_B \nu_B$$

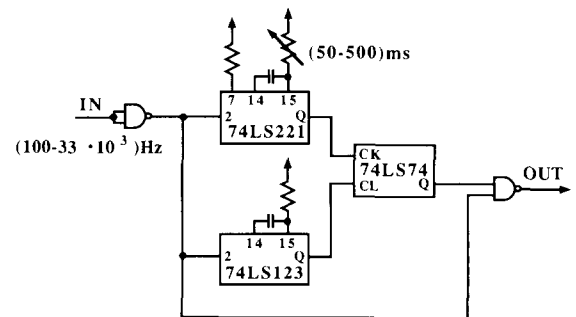


Fig. 5. Variable delay circuit permitting the time-shift mechanism.

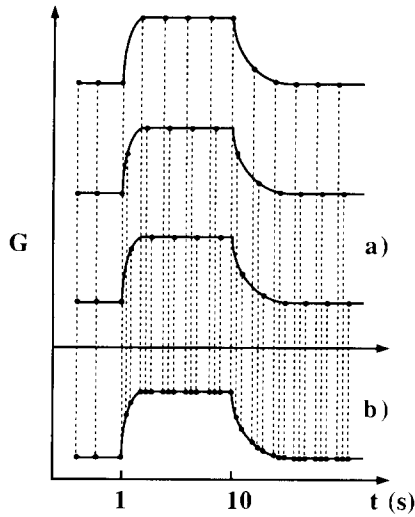


Fig. 6. Time-shift mechanism in the excitation cycle for short term rate effect. Measurements are iterated by setting an increasing delay each time (a). The final gain variation is obtained by overlap of every measurement (b).

for different combinations of charges Q_B , and pulse frequencies ν_B .

The raise of the PMT's gain to the excited level ΔG_{\max} is represented by the time dependence

$$\Delta G(t) = \Delta G_{\max}(1 - e^{-t/\tau_c}). \quad (1)$$

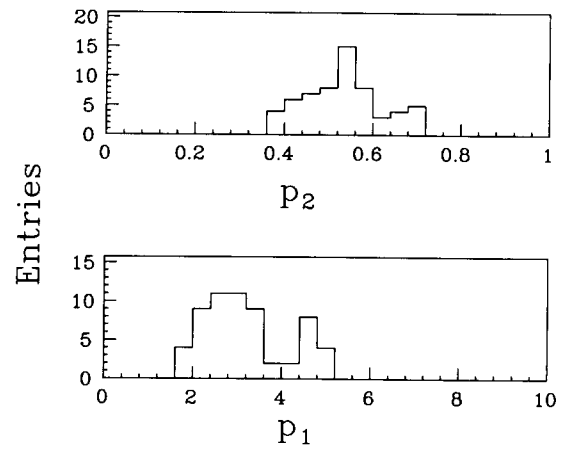


Fig. 8. Distribution of p_1 and p_2 parameters.

Similarly, at the end of the burst, the original level is reached with a time dependence

$$\Delta G(t) = \Delta G_{\max} e^{-t/\tau_r}. \quad (2)$$

Quantities ΔG_{\max} , τ_c and τ_r have been measured as functions of I , at five different values of Q_B :

$$Q_B = n(Q_B)_0, \quad n = 1 \text{ to } 5.$$

The anode charge $(Q_B)_0$ is due to $N_B \sim 10^4$ photoelec-

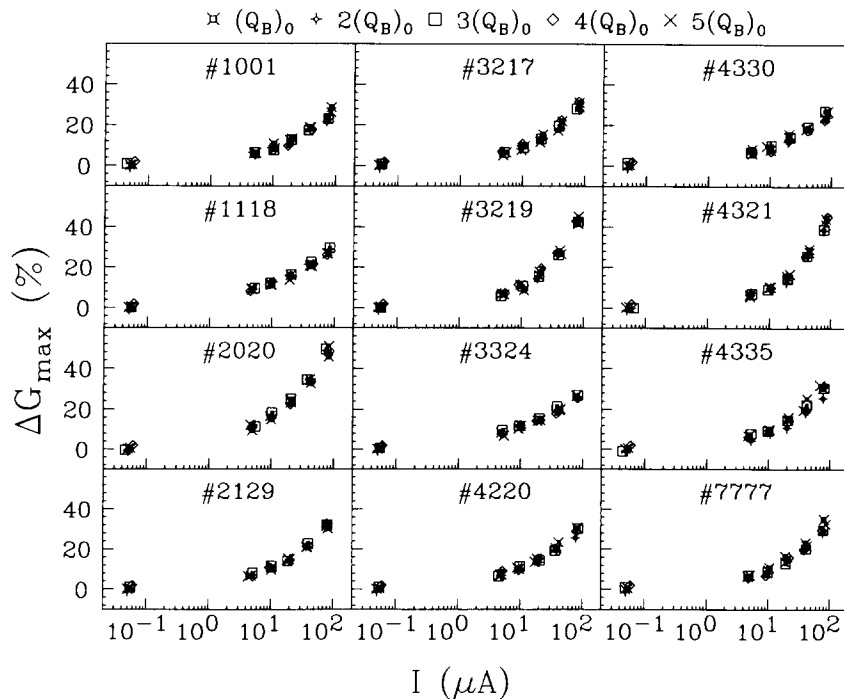
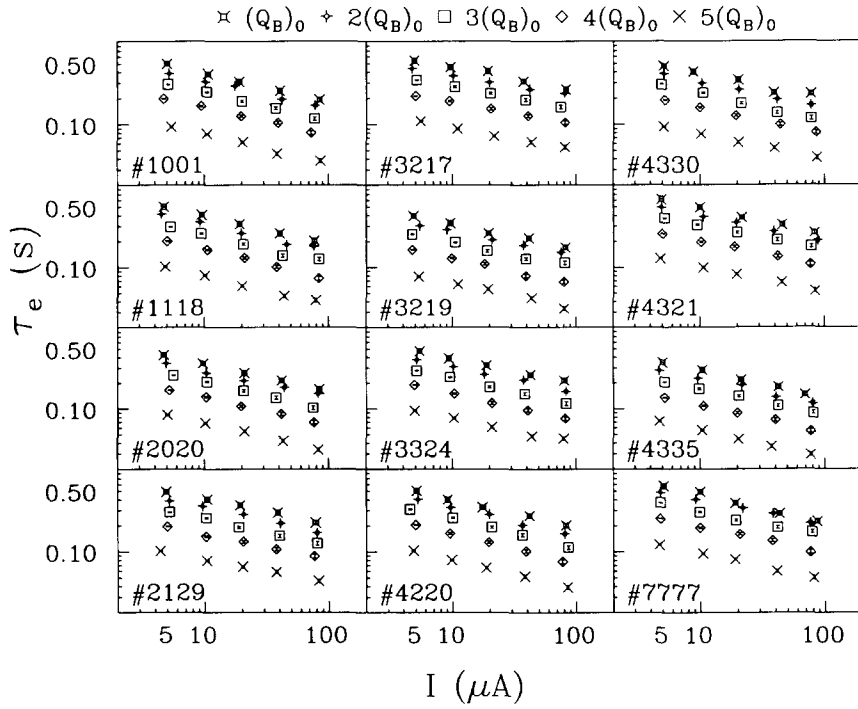
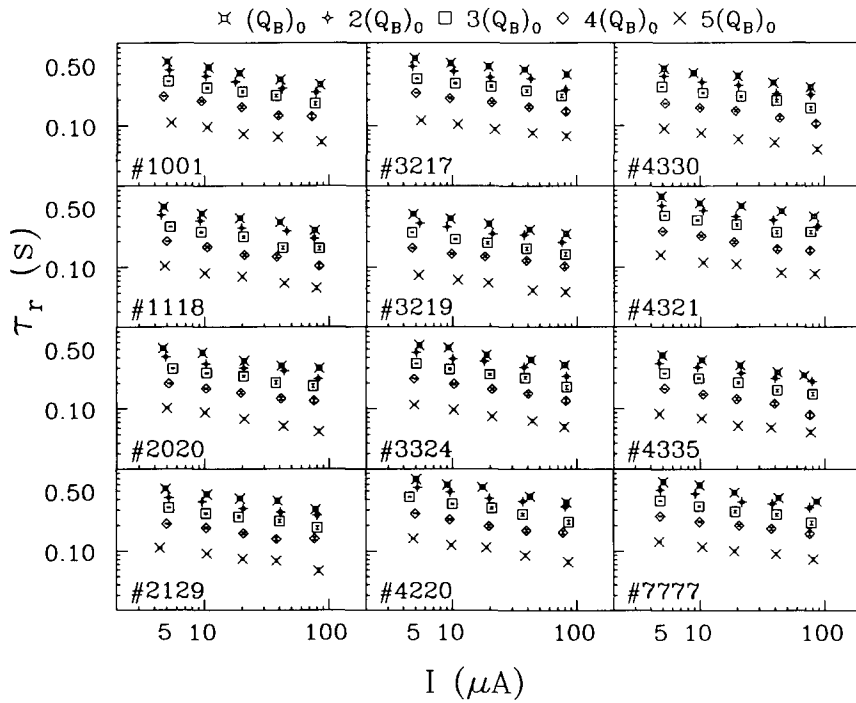


Fig. 7. Gain variation as a function of I and Q_B .

Fig. 9. Excitation times as functions of I and Q_B .

trons, and corresponds to about 2500 pC in absence of the rate effect, keeping the high voltage at $HV = -1680$ V.

For each specimen, the gain variation ΔG_{\max} appears to be independent on how Q_B and ν_B are combined to form the same I , within the experimental errors (fig. 7).

Fig. 10. Relaxation times as functions of I and Q_B .

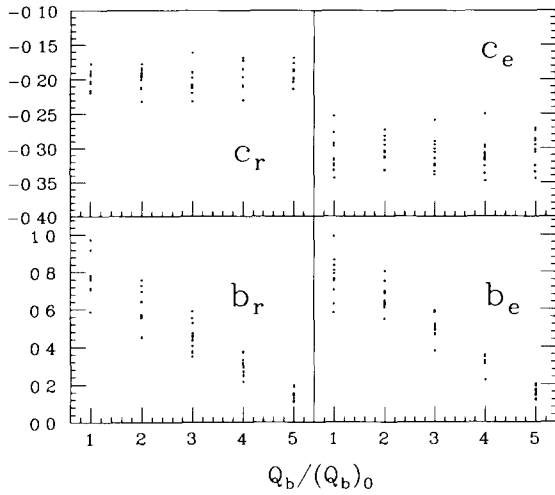


Fig. 11. Distribution of parameters $b_{e,r}$ and $c_{e,r}$, at constant HV.

Therefore, ΔG_{\max} is parametrized as a function of I only, by the law

$$\Delta G_{\max} = p_1 I^{p_2}. \quad (3)$$

Parameters p_1 and p_2 are computed by means of the best fit of the experimental points: fig. 8 shows their distributions for the sample of 12 PMTs tested. We find

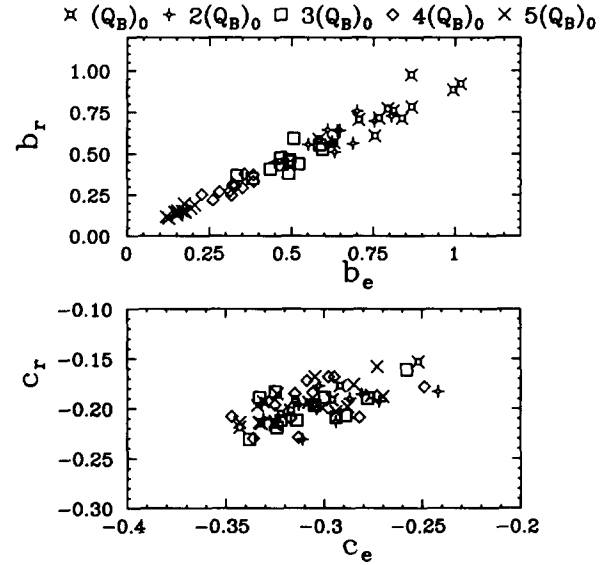


Fig. 12. Correlations between excitation and relaxation parameters $b_{e,r}$ and $c_{e,r}$ at constant HV.

for our sample of 12 PMTs values for exponents $0.4 \leq p_2 \leq 0.7$.

Excitation and relaxation times τ_r , τ_e are plotted as functions of I and Q_B in figs. 9 and 10, showing a decrease when I is increased; furthermore, a dependence on Q_B is also evident, as high Q_B correspond to

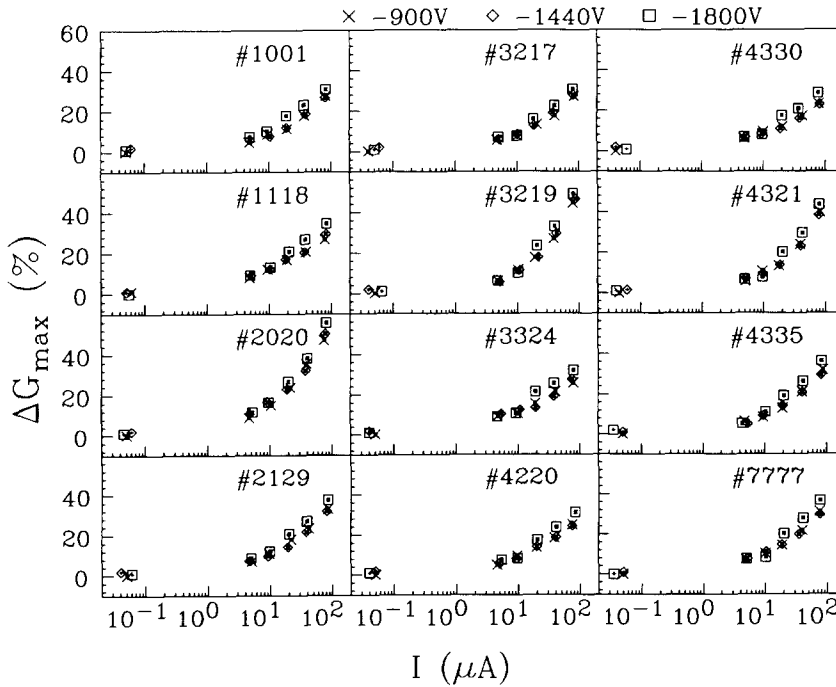
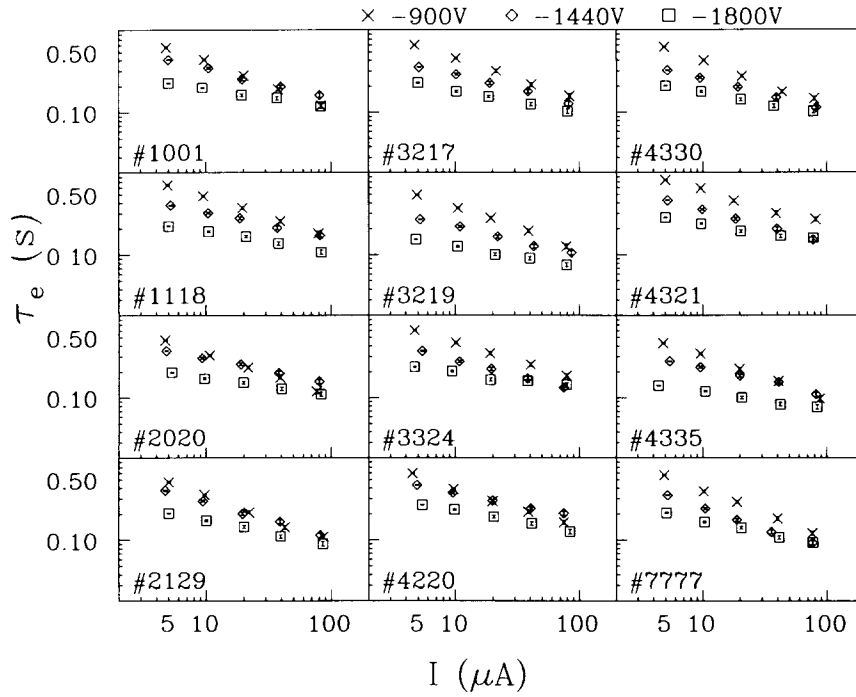


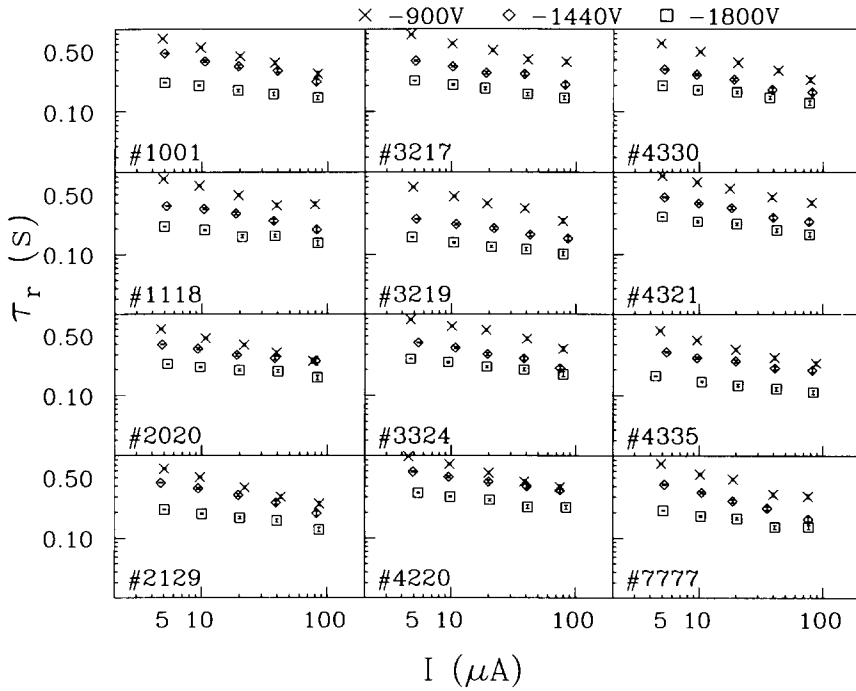
Fig. 13. Gain variation as a function of I and HV

Fig. 14. Excitation times as functions of I and HV.

low $\tau_{r,e}$. The dependence of $\tau_{e,r}$ on I and Q_B is well approximated by the law

$$\tau_{e,r} = \frac{b_{e,r}}{I^{c_{e,r}}} \quad (4)$$

Fig. 11 shows the distribution of the parameters $b_{e,r}$ and $c_{e,r}$ obtained from the best fit of eq. (4) to the data. Scale coefficients $b_{e,r}$ show a similar inverse proportionality on Q_B , while exponents $c_{e,r}$ do not depend on

Fig. 15. Relaxation times as functions of I and HV.

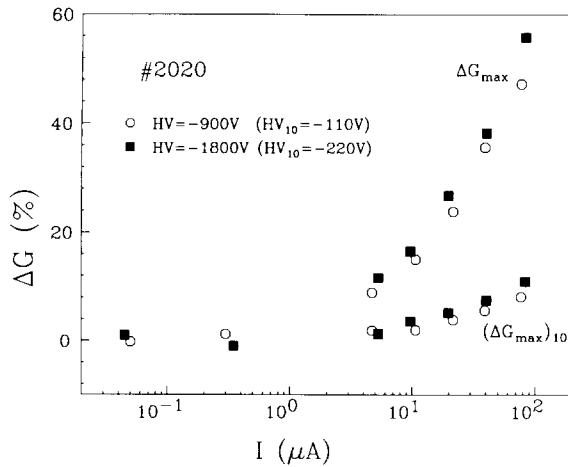


Fig. 16. The contribution of the last dynode $(\Delta G_{\max})_{10}$ to the overall gain variation ΔG_{\max} . Measurements have been repeated for two values of the tenth multiplicative stage voltage drop.

Q_B . Fig. 12 shows the correlation between parameters b and c in eq. (4).

Measurements have been repeated for three different values of the high voltage supply ($HV = -900, -1680, -1800$ V) keeping the anode charge constant [$Q_B = 3(Q_B)_0$]. A slight dependence of ΔG_{\max} on HV has been found; the variation is $\sim 5\%$ at $80 \mu A$ between -900 V and -1800 V (fig. 13). A dependence has also been found for $\tau_{e,r}$: the time necessary to reach (and to leave) the excited state characterized by ΔG_{\max} , diminishes for higher supply voltages (figs. 14 and 15).

By the measurements illustrated so far we have investigated the overall rate effect, i.e. that due to the sum of gain variations from all amplification stages. Nevertheless, some authors [4] claim that the rate effect should be explained as due mainly to the last dynode, through an enhanced conductivity mechanism.

Table 1

Compilation of data on the short term rate effect. Columns 5 to 10 show the qualitative behaviour of transition times when mean anode currents, anode charges and HV are increased. Transition times are found decreasing (\downarrow) or not depending (ND) on those quantities.

Reference	PMT model	n PMTs	p_2	$\tau_e(I)$	$\tau_r(I)$	$\tau_e(Q_a)$	$\tau_r(Q_a)$	$\tau_e(HV)$	$\tau_r(HV)$	$(\Delta G)_{1-9} : \Delta G$
[2]	FEU-84	32	"linear"	\downarrow	ND					
	FEU-85	16	"linear"	\downarrow	ND					
	FEU-110	3	"linear"	\downarrow	ND					
	FEU-115	16	"linear"	\downarrow	ND					
	XP2010	1	"linear"	\downarrow	ND					
[3]	XP2008	1	0.6							
[4]	XP2030	1	0.5–0.7	\downarrow	\downarrow	\downarrow	\downarrow	\downarrow	\downarrow	0.3 : 1
[5]	FEU-49B	1	0.3	\downarrow	\downarrow					0.97 : 1
	FEU-84-3	1	0.6	\downarrow	\downarrow					0.9 : 1
[10]	XP2972	3456	0.7							
This article	XP2008	12	0.4–0.7	\downarrow	\downarrow	\downarrow	\downarrow	\downarrow	\downarrow	0.8 : 1

To isolate the contribution of the last (tenth) dynode to the overall gain variation, we have used a subtraction method. Both voltage divider and readout circuitry were modified by supplying the anode with the same voltage as the tenth dynode, leaving all remaining voltage drops unchanged. In this configuration the PMT acts as a 9-dynode device, and gain variations due to the tenth dynode $(\Delta G_{\max})_{10}$ are isolated comparing results in both supply schemes:

$$(\Delta G_{\max})_{10} = \Delta G_{\max} - (\Delta G_{\max})_{1-9}.$$

Fig. 16 shows the separate contributions to the gain variation of the whole multiplicative chain, and of the last stage only. Such measurements have been done at HV supplies corresponding to cathode–anode voltage drops of -900 V and -1800 V respectively, in the ten-dynode configuration.

The last dynode appears to account for only about 20% of the total gain variation: we find indeed

$$\Delta G_{\max} / (\Delta G_{\max})_{1-9} = 1/0.8.$$

4. Concluding remarks

We have extensively studied a relevant sample of XP2008 PMTs, determining their most significant parameters in rate effect conditions. The rate effect has been studied under experimental conditions typical of particle accelerators, with on–off structures in the seconds domain (short-term rate effect).

We have shown that the gain variation is a function of the average anode current in the PMT, and does not depend separately on the amplitude nor on the frequency of the light pulses impinging on the photocathode. All stages in the PMT's multiplicative chain contribute similarly to the overall effect. We do not observe any magnification of the effect at the last dynode.

Transition times to the new "excited" working state, and from there back to ordinary conditions, depend

inversely on both the amplitude of light pulses on the photocathode (i.e. the anode charge), and the mean current flowing in the PMT. An analytical relationship has been found between transition times and those two quantities (4). Provided the mean current is kept constant, we also found that while the gain variation is practically independent of the operating HV, there is an inverse relationship between transition times and voltage supply applied.

Only one paper [3] has been published on the same PMT model, but it is confined to a limited set of measurements, and besides investigating only one specimen. To make a comparison of global trends, only a few articles are available concerning similar PMTs studied under short-time rate effect. We report in table 1 a compilation of available data compared with ours.

General agreement is found in the literature on gain variations as not depending separately on the pulse frequency and amplitude, but only on their product. Gain variations are directly proportional to the anode current: absolute values for samples studied in the literature are quite different from PMT to PMT, ranging from $\sim 10\%$ to $\sim 60\%$ at a mean anode current of $\sim 50 \mu\text{A}$.

We found the dependence of the gain variation on the average anode current well represented by a power-log law, with exponent in the range of 0.4–0.7, depending on the specimen. This parameter seems to be fairly well reproduced by all available measurements, considering the wide range of characteristics for the PMTs studied.

A quantitative comparison with the only other result on XP2008 [3] is difficult, since no description is given therein on what on/off cycle was used. Nevertheless, when we parametrise their data as functions of the mean anode current, the gain variation can be described as well by a power-log law, with exponent $p_2 \sim 0.6$.

Data has been published previously [2,4,5] on the time necessary for the PMT's gain to reach and leave the new state, at the beginning and end of the light burst. We found such times to be inversely correlated to the anode current, namely high current corresponds to fast times. Moreover we pointed out that, for a given anode current, transition times are shorter when the amplitude of the light pulse is larger. A similar behaviour has been shown in ref. [5] on FEU PMTs. However, an early study [2] on FEU PMTs claimed that a correlation similar to ours exists only for excitation times, but not for relaxation times.

The authors of ref. [4] have found a behaviour qualitatively comparable to ours, however isolating the contribution due to the last dynode only. Quantitative comparison is thus not possible.

Finally, our results on the relative contributions of different amplification stages to the rate effect show that the gain variation due to the multiplicative chain with the last dynode excluded is approximately in the

ratio 0.8:1 when compared to the gain variation due to the whole chain. Substantial agreement is found with ref. [5], claiming a ratio of 0.9:1.

These results suggest that the last dynode is not the main contribution to the phenomena, as often claimed in the literature, but instead all dynodes contribute with a comparable effect. Surprisingly, disagreement is found on this issue with ref. [4] on XP2030 PMTs. The relative contribution found is about 0.3:1. The authors explained this result with an electron enhanced conductivity of the dynodic oxide surface model, which predicts a larger effect on the last dynode, where a larger number of electrons are extracted. Such a model is not adequate to describe our data, and suggests that the mechanism could be more complicated.

Comparison between the results presented in this article and the available data in literature shows that, whilst a general agreement is found concerning the qualitative aspects of the rate effect phenomenology in the pulsed regime, it is not possible to describe all results within a general model yet.

Moreover, the influence of the specific on–off cycle adopted needs to be further clarified, in order to allow both a meaningful comparison between various authors' measurements, and a general way of relating the PMT's behaviour under rate effect conditions to the manufacturer's specifications.

Acknowledgements

Thanks are due to F. Bertino for his accurate CAD processing of line drawings. We gratefully acknowledge the contribution of L. Daniello and M. Giardoni, whose technical skills made the PMT's test apparatus possible.

References

- [1] I. Cantarell and L. Almodóvar, *Nucl. Instr. and Meth.* 24 (1963) 353.
- [2] G.A. Akopdzhanov et al., *Nucl. Instr. and Meth.* 161 (1979) 247.
- [3] F. Celani et al., *Nucl. Instr. and Meth.* 190 (1981) 71.
- [4] M. De Vincenzi et al., *Nucl. Instr. and Meth.* 225 (1984) 104.
- [5] V.N. Evdokimov and M.I. Mutafyan, *Instr. Exp. Tech.* 29 (1986) 900.
- [6] S. Bianco et al., A computer controlled system for testing large quantities of photomultiplier tubes, INFN Frascati LNF-85/49(R)(1985)
- [7] G. Bologna et al., *Nucl. Instr. and Meth.* 192 (1982) 315.
- [8] R. Baldini-Celio et al., *Nucl. Instr. and Meth.* 180 (1981) 249.
- [9] S. Cittolin and B.G. Taylor, *CAVIAR User Manual*, DD/OC/GA/80-2(1980).
- [10] M. Bonesini et al., *Nucl. Instr. and Meth.* A264 (1988) 205.